Search for Higgs Boson Pair Production in the $b\bar{b}\tau^+\tau^-$ Final State with the ATLAS Detector

Christopher Deutsch (on behalf of the ATLAS collaboration)

October 19, 2021

University of Bonn

Higgs Boson Pair Production

Non-Resonant Production

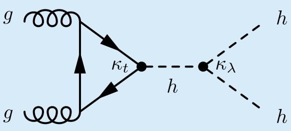

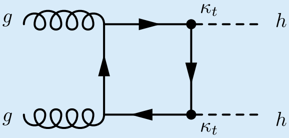

Resonant Production

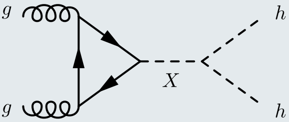

- Direct measurement of self-coupling κ_λ $\rightarrow$ access to Higgs potential
- Small cross section $\sigma_{HH}^{\text{ggF}} = 31.05\,\text{fb}^{\,*}$ in SM due to destructive interference
  - VBF contribution $\sigma_{HH}^{\text{VBF}} = 1.726\,\text{fb}^{\,\dagger}$ also considered

- Resonant enhancement in BSM scenarios
- Benchmark model:

  Narrow-width CP-even scalar X

  $251\,\text{GeV} \leq m_X \leq 1.6\,\text{TeV}$

*: NNLO QCD, $m_h = 125$ GeV, pp @ 13 TeV, J. High Energ. Phys. **2018**, 59 (2018)

†: N^{3}LO QCD, $m_h = 125$ GeV, pp @ 13 TeV, Phys. Rev. D **98**, 114016

The $b\bar{b}\tau^+\tau^-$ Final State

Di-Higgs Branching Ratios

	$b\bar{b}$	W^+W^-	$\tau^+\tau^-$	ZZ^*	$\gamma\gamma$
$b\bar{b}$	34 %				
W^+W^-	25 %	4.6 %			
$\tau^+\tau^-$	**7.3 %**	2.7 %	0.39 %		
ZZ^*	3.1 %	1.1 %	0.33 %	0.069 %	
$\gamma\gamma$	0.26 %	0.097 %	0.028 %	0.012 %	0.00052 %

BR for $m_h = 125$ GeV from LHCHXSWG

Di-Tau Branching Ratios

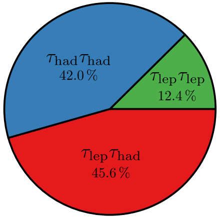

BR from PDG

- $HH \rightarrow b\bar{b}\tau^+\tau^-$ third largest BR of relevant channels
- High sensitivity to SM Higgs pair production
- Targeting semi-leptonic ($\tau_{lep}\tau_{had}$) and fully hadronic ($\tau_{had}\tau_{had}$) di-tau final states

Event Selection

$\tau_{had}\tau_{had}$	$\tau_{lep}\tau_{had}$ (SLT)	$\tau_{lep}\tau_{had}$ (LTT)
single & di-τ_{had} triggers	single ℓ triggers	$\ell + \tau_{had}$ triggers
exactly two τ_{had}	exactly one τ_{had} & one e or μ	
lepton-veto	$m_{bb} < 150$ GeV	
trigger-dependent thresholds on $e/\mu/\tau_{had}$ and jets		
$m_{\tau\tau}^{MMC} > 60$ GeV		
2 b-tagged jets		
OS el. charge of $\tau_e/\tau_\mu/\tau_{had}$ and τ_{had}		

Acceptance of non-res. *HH* (SM):

Channel	$(\mathcal{A} \times \varepsilon)^{ggF+VBF}_{SM\ HH}$
$\tau_{had}\tau_{had}$	4 %
$\tau_{lep}\tau_{had}$ (SLT)	4 %
$\tau_{lep}\tau_{had}$ (LTT)	1 %

ATLAS-CONF-2021-030

ATLAS-CONF-2021-030

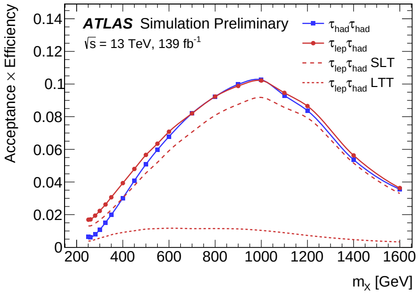

Event Selection

sin

- Close to two-fold improvement in signal acceptance compared to previous publication

  (Phys. Rev. Lett. **121**, 191801)

- Driven by improved reconstruction and identification of τ_{had} and b-jets

  (ATL-PHYS-PUB-2017-003, ATL-PHYS-PUB-2017-013, ATL-PHYS-PUB-2019-033)

Acceptance of non-res. *HH* (SM):

Channel	$(\mathcal{A} \times \varepsilon)^{\text{ggF+VBF}}_{\text{SM } HH}$
$\tau_{\text{had}}\tau_{\text{had}}$	4 %
$\tau_{\text{lep}}\tau_{\text{had}}$ (SLT)	4 %
$\tau_{\text{lep}}\tau_{\text{had}}$ (LTT)	1 %

ATLAS-CONF-2021-030

ATLAS-CONF-2021-030

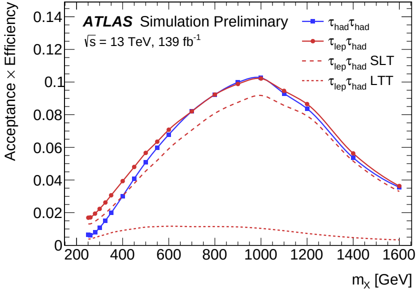

Background Estimation

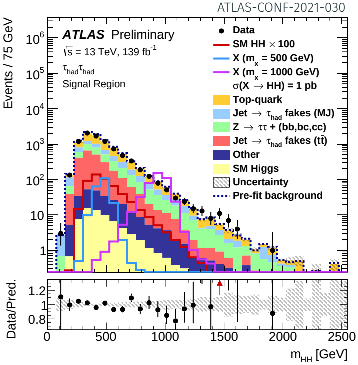

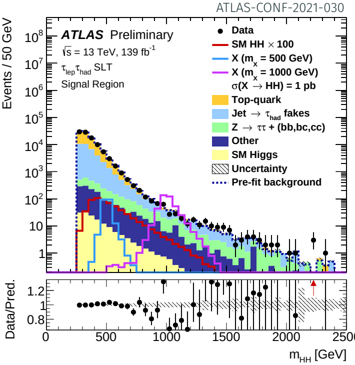

Background	$\tau_{had}\tau_{had}$-channel	$\tau_{lep}\tau_{had}$-channel
$t\bar{t}$	Simulation (normalized in fit)	
Z+jets	Simulation (normalized in fit – dedicated CR)	
jet $\to \tau_{had}$ fakes ($t\bar{t}$)	Simulation (data-driven mis-ID eff.)	Combined fake-factor method
jet $\to \tau_{had}$ fakes (multi-jet)	Fake-factor method	
SM Higgs / Other	Simulation	

Signal Extraction: Non-Resonant Higgs Pair Production

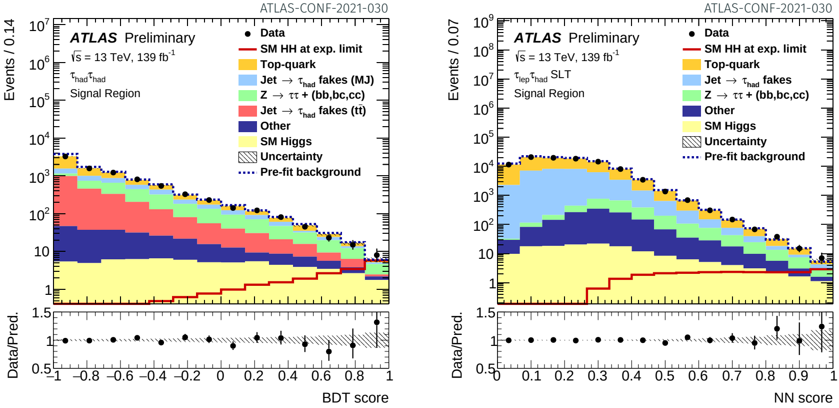

- Signal / background classifiers provide discriminant for likelihood fit

  $\tau_{had}\tau_{had}$: Boosted Decision Trees $\qquad$ $\tau_{lep}\tau_{had}$: Neural Networks

- Trained on signal vs. all backgrounds using high-level variables: E.g. m_{HH}, m_{bb}, $m_{\tau\tau}^{MMC}$, $\Delta R(\tau,\tau)$, . . .

Signal Extraction: Resonant Higgs Pair Production

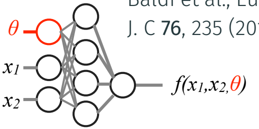

Baldi et al., Eur. Phys. J. C **76**, 235 (2016).

- Approach similar to non-resonant case
- Parametrized neural networks (PNN) used as discriminant
  - Parametrized in mass of scalar ($\theta = m_X$)
- Provides single classifier (per channel) for all considered m_X

ATLAS-CONF-2021-030

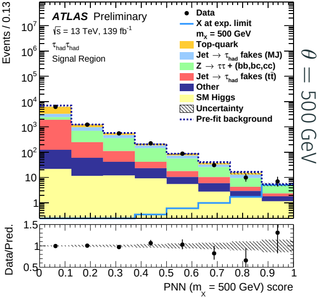

ATLAS-CONF-2021-030

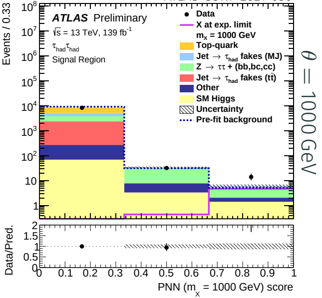

Uncertainties

- Uncertainty on signal strength statistically dominated
- Leading systematic sources (non-res. HH):
  - MC statistics
  - Top / Single Higgs modelling

Search for $X \to HH$:

- Similar picture
- Depending on m_X: Fake-τ_{had}, Z+jets, signal modeling up to 30 %

Relative uncertainty explained by source:

Uncertainty source	Non-resonant HH
Data statistical	81%
Systematic	59%
$t\bar{t}$ and Z + HF normalisations	4%
MC statistical	28%
Experimental	
Jet and $E_{\text{T}}^{\text{miss}}$	7%
b-jet tagging	3%
$\tau_{\text{had-vis}}$	5%
Electrons and muons	2%
Luminosity and pileup	3%
Theoretical and modelling	
Fake-$\tau_{\text{had-vis}}$	9%
Top-quark	24%
$Z(\to \tau\tau)$ + HF	9%
Single Higgs boson	29%
Other backgrounds	3%
Signal	5%

ATLAS-CONF-2021-030

$$\frac{\sqrt{\Delta\mu^2_{\text{tot}} - \Delta\mu^2_{\text{categ.-fixed}}}}{\Delta\mu_{\text{tot}}}$$

Results & Conclusion

Cross section upper limits on

$pp \to HH$ (non-resonant)

$pp \to X \to HH$ (resonant)

ATL-PHYS-PUB-2021-031

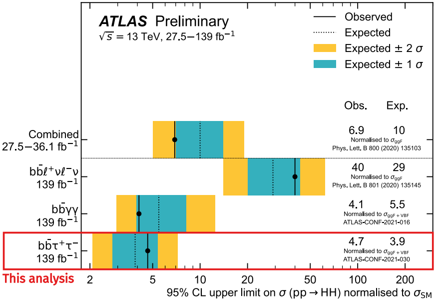

ATLAS-CONF-2021-030

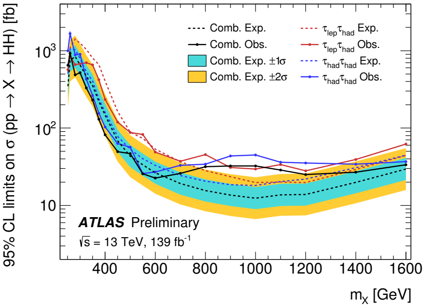

- Upper limit on $\sigma_{HH}^{\text{ggF+VBF}}$: obs. $4.7 \times \sigma_{\text{SM}}$ (exp. $3.9 \times \sigma_{\text{SM}}$)
  - Highest expected sensitivity to date
- Upper limits on $\sigma_{X \to HH}$ for narrow-width scalars ranging from approx. 20–10^3 fb
  - Largest excess at 1 TeV with local (global) significance of 3.0σ (2.0σ)

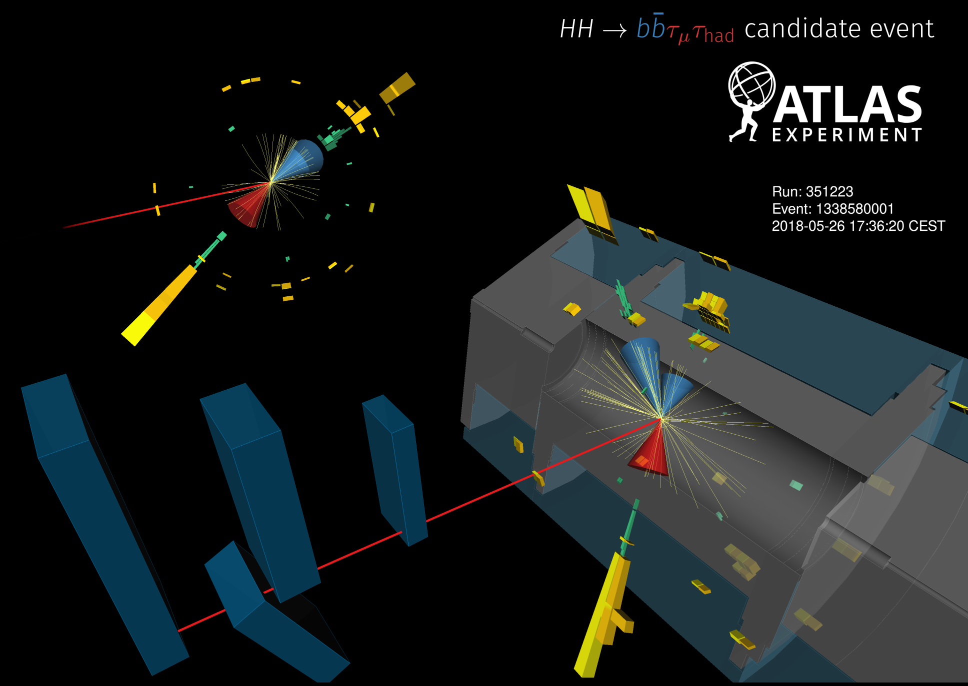

ATLAS-CONF-2021-030

$HH \rightarrow b\bar{b}\tau_{\text{had}}\tau_{\text{had}}$ candidate event

Run: 339535
Event: 996385095
2017-10-31 00:02:20 CEST

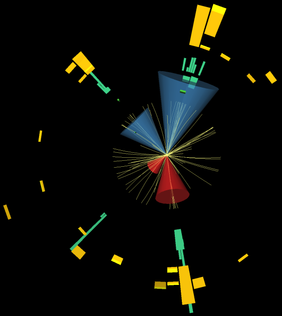

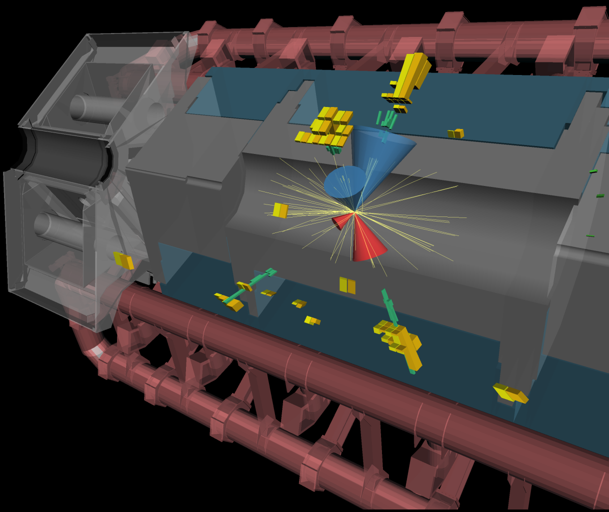

ATLAS-CONF-2021-030

Discussion Session

Summary for Discussion Session

Non-Resonant Production

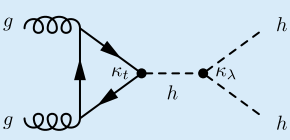

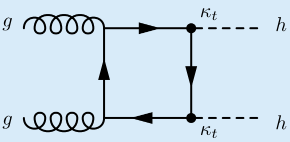

Resonant Production

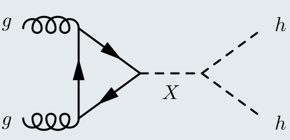

ATL-PHYS-PUB-2021-031

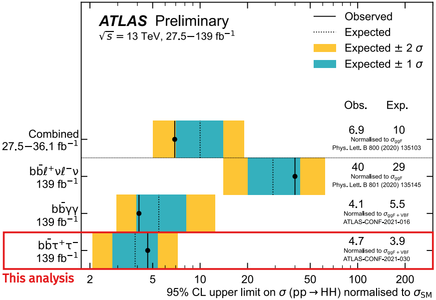

ATLAS-CONF-2021-030

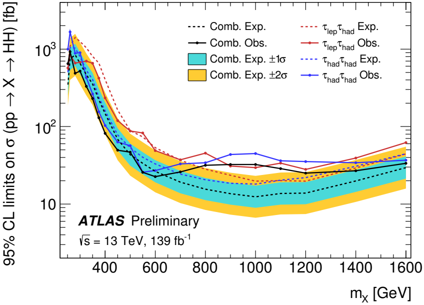

Backup

Selection

$\tau_{\text{had}}\tau_{\text{had}}$ category		$\tau_{\text{lep}}\tau_{\text{had}}$ categories	
STT	DTT	SLT	LTT
e/μ selection			
No loose e/μ with $p_{\text{T}} > 7$ GeV		Exactly one tight e or medium μ	
		$p_{\text{T}}^{e} > 25, 27$ GeV	18 GeV $< p_{\text{T}}^{e} <$ SLT cut
		$p_{\text{T}}^{\mu} > 21, 27$ GeV	15 GeV $< p_{\text{T}}^{\mu} <$ SLT cut
		$\lvert\eta^{e}\rvert < 2.47$, not $1.37 < \lvert\eta^{e}\rvert < 1.52$	
		$\lvert\eta^{\mu}\rvert < 2.7$	
$\tau_{\text{had-vis}}$ selection			
Two loose $\tau_{\text{had-vis}}$		One loose $\tau_{\text{had-vis}}$	
$\lvert\eta\rvert < 2.5$		$\lvert\eta\rvert < 2.3$	
$p_{\text{T}} > 100, 140, 180$ (25) GeV	$p_{\text{T}} > 40$ (30) GeV	$p_{\text{T}} > 20$ GeV	$p_{\text{T}} > 30$ GeV
Jet selection			
≥ 2 jets with $\lvert\eta\rvert < 2.5$			
$p_{\text{T}} > 45$ (20) GeV	Trigger dependent	$p_{\text{T}} > 45$ (20) GeV	Trigger dependent
Event-level selection			
Trigger requirements passed			
Collision vertex reconstructed			
$m_{\tau\tau}^{\text{MMC}} > 60$ GeV			
Opposite-sign electric charges of $e/\mu/\tau_{\text{had-vis}}$ and $\tau_{\text{had-vis}}$			
Exactly two b-tagged jets			
		$m_{bb} < 150$ GeV	

ATLAS-CONF-2021-030

MVA Input Variables

Variable	$\tau_{\text{had}}\tau_{\text{had}}$	$\tau_{\text{lep}}\tau_{\text{had}}$ SLT	$\tau_{\text{lep}}\tau_{\text{had}}$ LTT
m_{HH}	✓	✓	✓
$m_{\tau\tau}^{\text{MMC}}$	✓	✓	✓
m_{bb}	✓	✓	✓
$\Delta R(\tau, \tau)$	✓	✓	✓
$\Delta R(b, b)$	✓	✓	
$\Delta p_{\text{T}}(\ell, \tau)$		✓	✓
Sub-leading b-tagged jet p_{T}		✓	
m_{T}^{W}		✓	
$E_{\text{T}}^{\text{miss}}$		✓	
$\mathbf{p}_{\text{T}}^{\text{miss}}$ ϕ centrality		✓	
$\Delta\phi(\tau\tau, bb)$		✓	
$\Delta\phi(\ell, \mathbf{p}_{\text{T}}^{\text{miss}})$			✓
$\Delta\phi(\ell\tau, \mathbf{p}_{\text{T}}^{\text{miss}})$			✓
S_{T}			✓

ATLAS-CONF-2021-030

Uncertainty Breakdown

Table 4: Breakdown of the relative contributions to the uncertainty in the extracted signal cross-sections, as determined in the likelihood fit to data. These are obtained by fixing the relevant nuisance parameters in the likelihood fit, and subtracting the obtained uncertainty on the fitted signal cross-sections in quadrature from the total uncertainty, and then dividing the result by the total uncertainty. The sum in quadrature of the individual components differs from the total uncertainty due to correlations between the groups of uncertainties.

Uncertainty source	Non-resonant HH	Resonant $X \to HH$		
		300 GeV	500 GeV	1000 GeV
Data statistical	81%	75%	89%	88%
Systematic	59%	66%	46%	48%
$t\bar{t}$ and Z + HF normalisations	4%	15%	3%	3%
MC statistical	28%	44%	33%	18%
Experimental				
Jet and $E_{\mathrm{T}}^{\mathrm{miss}}$	7%	28%	5%	3%
b-jet tagging	3%	6%	3%	3%
$\tau_{\text{had-vis}}$	5%	13%	3%	7%
Electrons and muons	2%	3%	2%	1%
Luminosity and pileup	3%	2%	2%	5%
Theoretical and modelling				
Fake-$\tau_{\text{had-vis}}$	9%	22%	8%	7%
Top-quark	24%	17%	15%	8%
$Z(\to \tau\tau)$ + HF	9%	17%	9%	15%
Single Higgs boson	29%	2%	15%	14%
Other backgrounds	3%	2%	5%	3%
Signal	5%	15%	13%	34%

ATLAS-CONF-2021-030

Additional Plots for SLT

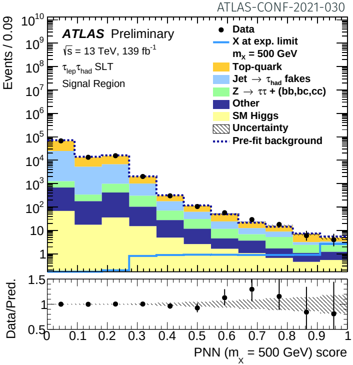

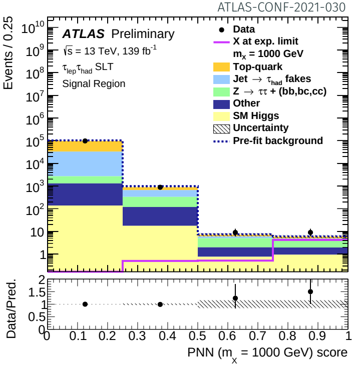

Additional Plots for LTT (1)

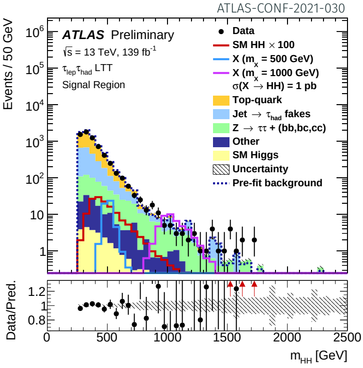

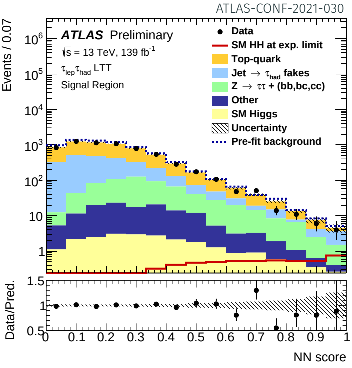

Additional Plots for LTT (2)

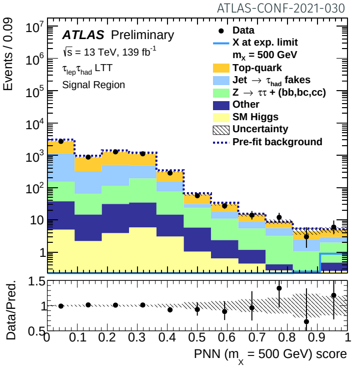

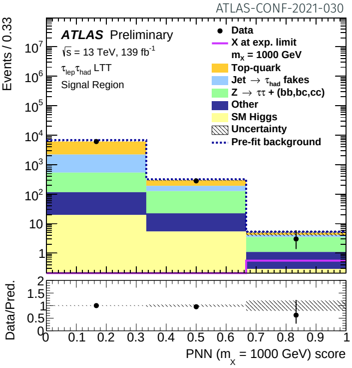

Non-Resonant HH Results

Table 5: Observed and expected upper limits at 95% CL on the cross-section of non-resonant HH production according to SM-like kinematics, and on the cross-section of non-resonant HH production divided by the SM prediction. The $\pm 1\ \sigma$ and $\pm 2\ \sigma$ variations around the expected limit are also shown.

		Observed	$-2\ \sigma$	$-1\ \sigma$	Expected	$+1\ \sigma$	$+2\ \sigma$
$\tau_{\text{had}}\tau_{\text{had}}$	$\sigma_{\text{ggF+VBF}}$ [fb]	145	70.5	94.6	131	183	245
	$\sigma_{\text{ggF+VBF}}/\sigma^{\text{SM}}_{\text{ggF+VBF}}$	4.95	2.38	3.19	4.43	6.17	8.27
$\tau_{\text{lep}}\tau_{\text{had}}$	$\sigma_{\text{ggF+VBF}}$ [fb]	265	124	167	231	322	432
	$\sigma_{\text{ggF+VBF}}/\sigma^{\text{SM}}_{\text{ggF+VBF}}$	9.16	4.22	5.66	7.86	10.9	14.7
Combined	$\sigma_{\text{ggF+VBF}}$ [fb]	135	61.3	82.3	114	159	213
	$\sigma_{\text{ggF+VBF}}/\sigma^{\text{SM}}_{\text{ggF+VBF}}$	4.65	2.08	2.79	3.87	5.39	7.22

ATLAS-CONF-2021-030